Beamforming Techniques Applied in EEG Source Analysis

3 AUTHORS, INCLUDING:

Rik Van de Walle
Ghent University
704 PUBLICATIONS **4,216** CITATIONS

SEE PROFILE

Bart Vanrumste
University of Leuven
134 PUBLICATIONS **1,466** CITATIONS

SEE PROFILE

Beamforming Techniques Applied in EEG Source Analysis

G. Van Hoey[1,2], R. Van de Walle[1], B. Vanrumste[1,2], M. D'Havé[2], I. Lemahieu[1] and P. Boon[2]

[1]Department of Electronics and Information Systems, University of Ghent
Sint-Pietersnieuwstraat 41, B-9000 Ghent, Belgium

[2]Epilepsy Monitoring Unit, Department of Neurology, University Hospital of Ghent

Tel. +32-9-240.43.85   Fax. +32-9-240.49.71
E-mail: gert.vanhoey@rug.ac.be

Abstract— **The electrical activity of the human brain causes time-varying potential differences on the head surface. The electroencephalogram (EEG) is a measurement of these potential differences between electrodes on the head. When the electrical brain activity is limited to a small region in the brain (e.g., during epileptic seizures), the source region within the brain can be localised by analysing the EEG. The estimated location of the source provides important additional information in the planning of a surgical treatment of the epilepsy [1, 2]. Beamforming techniques for spatial filtering, originally designed for applications in radar signal processing, are able to extract from the measured EEG signals, the source activity of a predefined region of interest within the brain. Depending on the way in which the weight factors of the beamformer are chosen, different beamformers can be constructed with different properties concerning spatial specificity and sensitivity to noise. By using simulated EEG signals, we have compared the performance of three beamformers (quiescent beamformer, linearly constrained minimum variance beamformer, and eigenspace-based beamformer). We conclude that the eigenspace-based beamformer performs best in extracting from the EEG the signal of the desired source, while offering a good suppression of measurement noise.**

I. Introduction

The electrical activity of the neurons in the brain cause time-varying potential differences on the surface of the head (scalp) that can be measured between electrodes. A measurement of these potential differences with electrodes positioned at standard locations on the head is an electroencephalogram (EEG). The EEG of patients with epilepsy is often featured by the presence of *interictal spikes*, which are short peaks with high amplitude originating from electrical activity in a limited area in the brain. During epileptic seizures, the EEG often shows rhythmic electrical activity arising from the same *epileptogenic* area in the brain.

Beamforming is a technique that performs a spatial filtering of signals measured at discrete sensors [3]. Beamformers calculate a linear combination of the time sequences measured at the different sensors, with the aim of preserving the signal components originating from a desired direction or location, while at the same time suppressing interference from other directions or locations. A typical application of beamforming is a spatial filtering of radar signals, in which the signal in a certain direction-of-arrival is to be extracted from the signals measured at a linear sensor array. Beamforming can be applied as well in cases with more general sensor configurations.

In EEG, beamforming can be applied to implement a spatial filter that monitors the electrical activity in a certain brain region, while suppressing the contributions of interfering activity in other regions. The use of beamforming in EEG was reported in [4, 5].

The behaviour of a beamformer (spatial response function, sensitivity to noise) is completely determined by the choice of its coefficients for linearly combining the input signals. Different types of beamformers exist, depending on the criteria put forward to determine their coefficients. In this paper, we consider three types of beamformers applied to EEG signals. We compare the different approaches with respect to suppression of interfering sources and sensitivity to background noise.

II. Theory

A. Dipole modelling of epileptic brain activity

The electrical activity in a limited brain area can adequately be modelled by a current dipole, which represents a current source within the conductive brain tissue. The parameters of a current dipole model are its location and its orientation. The location of the dipole represents the location of the active area within the brain for which it serves as a model. The orientation of the dipole represents the alignment of the brain cells in the active area.

The *forward problem* in EEG consists of the calculation of the potentials measured at the scalp electrodes, caused by a known electrical dipole source within the head.

The 6 parameters of a dipole source are its three coordinates in $\mathbf{r}_d \in \mathsf{R}^{3 \times 1}$ and its three dipole components in $\mathbf{d} = (d_x, d_y, d_x)^T \in \mathsf{R}^{3 \times 1}$ (or, equivalently, two orientation angles and one intensity parameter). For each possible dipole position $\mathbf{r}_d$ within the head, the relation between $\mathbf{d}$ and the potentials $\mathbf{v}_{mod} \in \mathsf{R}^{m \times 1}$ measured at the m electrodes can be written

$$\mathbf{v}_{mod} = \mathbf{L}(\mathbf{r}_d) \cdot \mathbf{d}. \qquad (1)$$

The matrix $\mathbf{L} \in \mathsf{R}^{m \times 3}$ is the *lead field matrix*, determined by dipole position, electrode positions, and head geometry.

A spherical model can be used for the head, consisting of a central sphere for the brain and two concentric spherical shells for the skull and scalp. In this case, an analytical expression exists for the lead field matrix $\mathbf{L}$ [6]. When analyzing patient EEG data, a more realistically shaped head model is often desirable, but in this case, numerical methods such as the boundary element or finite difference method are needed to calculate the lead field matrix [7,8].

B. Beamforming

If we denote the EEG signal measured at m electrodes during n time samples by the matrix $\mathbf{V} \in \mathsf{R}^{m \times n}$, the output $\mathbf{y} \in \mathsf{R}^{1 \times n}$ of a beamformer can be written as

$$\mathbf{y} = \mathbf{w}^T \mathbf{V}, \qquad (2)$$

where the vector $\mathbf{w} \in \mathsf{R}^{m \times 1}$ is the weight vector of the beamformer, containing the coefficients for linearly combining the signals measured at the electrodes. When applying beamforming for EEG signals, we typically want to extract the signal arising from a small area in the brain, which is modelled by a dipole at that location $\mathbf{r}_d$ having a certain orientation (with corresponding dipole components $\mathbf{d}$). Given this dipole and its components, equation (1) determines the corresponding potential distribution

$$\mathbf{c} = \mathbf{L}(\mathbf{r}_d) \cdot \mathbf{d} \qquad (3)$$

at the scalp electrodes, with $\mathbf{c} \in \mathsf{R}^{m \times 1}$. The desired property of the beamformer is translated into a prescription for determining $\mathbf{w}$ by requiring

$$\mathbf{w}^T \mathbf{c} = 1, \qquad (4)$$

which implies the constraint that any contribution of the considered dipole source to the measured EEG must be preserved with unity gain at the output of the beamformer. Equation (4) is a linear equation in the coefficients contained within $\mathbf{w}$, which obviously does not uniquely determine $\mathbf{w}$. Different additional requirements can be put forward to select one of the solutions of equation (4) as the weight vector $\mathbf{w}$, each leading to a different type of beamformer.

The output variance or output power of a beamformer is

$$\varepsilon\{|y(k)|^2\}, \quad k = -\infty, \ldots, \infty, \qquad (5)$$

where represents $\varepsilon\{\cdot\}$ the expected value of its argument, can be proven to equal

$$\mathbf{w}^T \mathbf{R}_v \mathbf{w}, \qquad (6)$$

with $\mathbf{R}_v$ the covariance matrix of the different EEG channels.

As a consequence, additive noise in the measurements that is uncorrelated over the different EEG channels has a contribution in the output power that equals $\mathbf{w}^T \mathbf{w}$. This type of noise is called spatially white. If no prior information is available on the interfering signal sources influencing the measurements, the weights $\mathbf{w}$ of the beamformer can be chosen as the solution to (4) having a minimum norm,

$$\mathbf{w}_Q = \mathbf{c}(\mathbf{c}^T \mathbf{c})^{-1}, \qquad (7)$$

yielding the beamformer with the smallest additive (spatially) white noise gain. This type of beamformer is called the *quiescent beamformer*. The quiescent beamformer is a data-independent beamformer because it does not exploit the information in the signals in $\mathbf{V}$ to characterize the interfering sources and choose the weights $\mathbf{w}$ accordingly.

A second type of beamformer is the *linearly constrained minimum variance (LCMV) beamformer*, which requires the weight vector to minimize the output power in equation (5), subject to equation (4) as a side constraint, i.e.

$$\min_{\mathbf{w}} \mathbf{w}^T \mathbf{R}_v \mathbf{w} \quad s.t. \quad \mathbf{w}^T \mathbf{c} = 1. \tag{8}$$

The following expression

$$\mathbf{w}_{LCMV} = \mathbf{R}_v^{-1} \mathbf{c} (\mathbf{c}^T \mathbf{R}_v^{-1} \mathbf{c})^{-1} \tag{9}$$

can be derived for the weights of the LCMV beamformer by constrained minimization using Lagrange multipliers. In practice, the matrix $\mathbf{R}_v$ will have to be estimated from a measurement of the EEG during a limited time interval as

$$\mathbf{R}_v = \frac{1}{n} \mathbf{V}^T \mathbf{V}. \tag{10}$$

The LCMV beamformer can be interpreted to extract the contribution of the desired dipole source with unity gain, while at the same time minimizing the overall output power, thus maximally suppressing contributions from other regions than the desired dipole. Through the use of the covariance matrix $\mathbf{R}_v$, the LCMV beamformer uses the information included in the signals $\mathbf{V}$ to determine the weights in $\mathbf{w}$ such that interferences are maximally reduced. It is clear that the norm of $\mathbf{w}_{LCMV}$ will in general be larger than the norm of $\mathbf{w}_Q$ which causes the LCMV beamformer to be more sensitive to additive white noise than the quiescent beamformer.

A third type of beamformer is the *eigenspace-based beamformer*, which makes use of dividing the m-dimensional measurement space into signal space and a noise space, based on $\mathbf{V}$. The beamformer uses as its weight vector the projection of $\mathbf{w}_{LCMV}$ onto the signal space. Because the signal and noise space are orthogonal complements, only the components of $\mathbf{V}$ lying in the signal space will influence the output of the eigenspace-based beamformer. Components of $\mathbf{V}$ in the noise space yield a zero output. As a result, the eigenspace-based beamformer typically has a lower white noise gain than the LCMV beamformer. Note, however, that due to the projection of the weight vector onto the signal space, equation (4) does generally not hold for the eigenspace-based beamformer. Dividing the measurement space into a signal and noise space can be performed by applying the singular value decomposition (SVD) on the measurement matrix $\mathbf{V} \in \mathsf{R}^{m \times n}$:

$$\mathbf{V} = \mathbf{P}^T \mathbf{S} \mathbf{Q}, \quad \mathbf{P} \in \mathsf{R}^{m \times m}, \mathbf{Q} \in \mathsf{R}^{n \times n}, \tag{11}$$

or, equivalently, an eigenspace decomposition of the matrix $\mathbf{V}^T \mathbf{V}$, hence the name eigenspace-based beamformer. The diagonal matrix $\mathbf{S}$ contains the singular values and would theoretically contain a few large singular values, corresponding with the number of active dipolar sources. The remaining singular values should have a low value and should all be equal to the noise variance σ^2. The number of large singular values determines the dimension of the signal space and the corresponding columns of $\mathbf{P}$ are a set of basis vectors that span the signal space.

III. Methods

A. Electrode placement and head model

In clinical practice, the EEG of epileptic patients is measured using 27 scalp electrodes. Therefore, the following experiments and simulations are performed using the corresponding 27 standard electrode positions on a spherical head model. This electrode placement is illustrated in figure 1. In the following experiments, we use a 3-shell spherical head model. The radii of the outer boundaries of the brain, skull and scalp are 8, 8.5 and 9.2 cm, respectively.
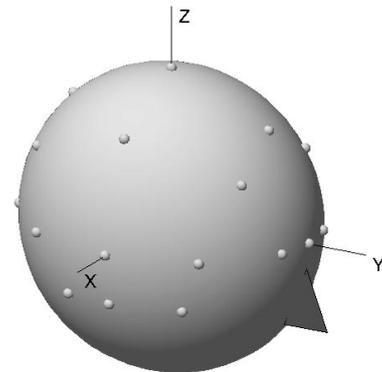

Fig. 1. Illustration of placement of the 27 EEG electrodes. The x, y, and z axes point towards the right, the front, and the top, respectively.

B. Simulation study

In this paper, we apply the different types of beamformer to simulated EEG signals, in order to study their ability to suppress interfering sources and white noise. The simulated signals are the superposition of the EEG caused by dipole 1, located at ($x = -0.5, y = 0, z = 0$), having a sinusoidal time variation of its intensity at f_1=10 Hz, and the EEG caused by dipole 2, located at ($x = 0.5, y = 0, z = 0$), having a sinusoidal time variation of its intensity at f_2=15 Hz.

Both dipole locations are illustrated in figure 2. Additionally, spatially white noise was added to the EEG. Figure 3 shows the simulated EEG at the 27 electrodes. While the potential at each electrode is a mixture of both components, the 10 Hz-activity can be observed most clearly at electrode 4, because the dipole orientation points approximately to the electrode's location. The 20 Hz-activity is best observed at electrode 12.
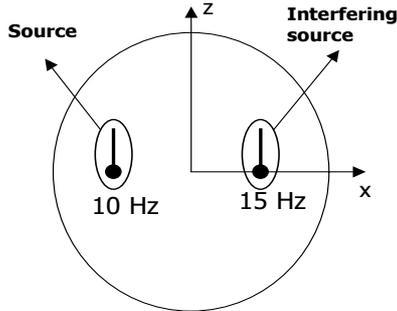

Fig. 2. Dipole positions for dipole 1 (source to be extracted) and dipole 2 (interfering source).
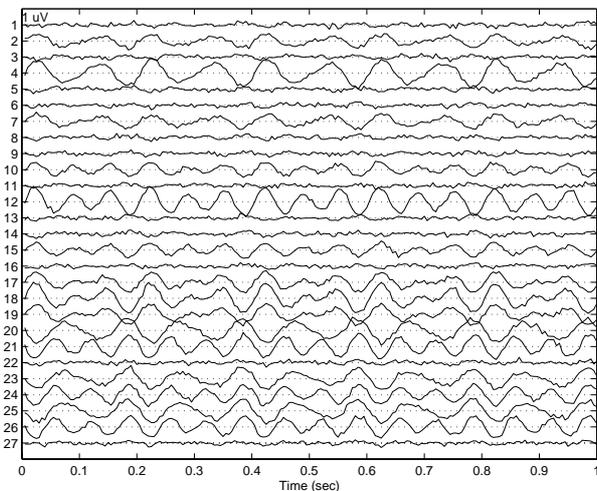

Fig. 3. Simulated EEG signals measured at the 27 electrodes.

Dipole 1 is the source for which the time-varying amplitude variation is to be extracted from the EEG signals. The location of dipole 1 is considered to be known, and thus, formula (3) can be used to calculate its corresponding potential distribution $\mathbf{c}_1$. Dipole 2 is considered as an interfering source, for which the location within the head model is unknown.

Each of the three beamformers was applied to the simulated EEG, and two measures were calculated to quantify their performance. The capability of the

beamformers to suppress the interfering source can be described by the *interference sensitivity (IS)*

$$IS = \frac{a_2^2}{a_1^2}, \qquad (12)$$

where a_1 and a_2 are defined by

$$a_i = \frac{\int y(t)\sin(2\pi f_i t)dt}{\sqrt{\int \sin^2(2\pi f_i t)dt}}, \quad i = 1, 2. \qquad (13)$$

IS measures the proportion of the 15 Hz interferer power to the 10 Hz source power in the beamformer's output.

The capability of the beamformers to suppress white noise is quantified by the *signal-to-noise ratio (SNR)*

$$SNR = \frac{a_1^2 + a_2^2}{P - a_1^2 - a_2^2}, \qquad (14)$$

where P is the output power of the beamformer, given by

$$P = \int y^2(t)dt. \qquad (15)$$

IV. RESULTS AND DISCUSSION

Figure 4 shows the output signals of the three beamformers, when the simulated EEG signals are applied to their input. The quiescent beamformer clearly does not succeed in suppressing the interfering 15 Hz source activity. In the output of the LCMV beamformer, the interfering source activity is strongly reduced. However, the LCMV beamformer output appears to be noisy. The LCMV beamformer has a considerably higher white noise gain than the quiescent beamformer, which has the lowest possible white noise gain, because $\mathbf{w}_Q$ is the minimum-norm solution of (4). The eigenspace-based beamformer strongly suppresses the interfering source as well, and has at the same time a low white noise gain. It can be observed, however, that the output signal of the eigenspace beamformer has a slightly lower amplitude than the original source activity. This is caused by the fact that, by projecting $\mathbf{w}_{LCMV}$ onto the signal space, the condition (4) is not preserved. The IS and SNR measures are given in table I and confirm the observations based on figure 4.

The results of this simulation clearly indicate that the eigenspace-based beamformer is superior to both the quiescent and the LCMV beamformer, as it combines a low white noise gain with a high suppression of the interfering source.
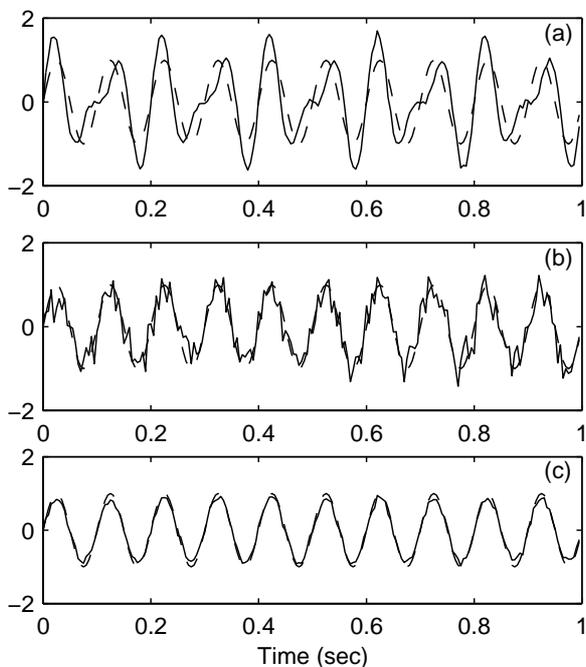
Fig. 4. Output signals from the quiescent (a), LCMV (b), and eigenspace-based (c) beamformers (solid line), together with the original amplitude of dipole source 1 (dashed line).

Type	IS	SNR
Quiescent beamformer	0.4707	273.492
LCMV beamformer	$1.323 \cdot 10^{-5}$	4.835
Eigenspace beamformer	$2.165 \cdot 10^{-5}$	109.994

TABLE I

VALUES OF THE INTERFERENCE SENSITIVITY AND SIGNAL-TO-NOISE RATIO FOR THE THREE BEAMFORMERS.

It should be emphasized, however, that the simulation used in this article is favourable for obtaining high beamformer performance, for two reasons. First, the potential distribution corresponding to the desired dipole was considered to be known. When analyzing real EEG, the location and orientation of the source activity to be extracted, will be known only approximately. And even if they were known, imperfections in the head model (e.g., using a spherical model for approximating a realistic geometry) will yield imperfect information about the potential distribution. Secondly, the separation of the measurement space into the signal and noise spaces was straightforward in our simulation, because the SVD produced two singular values that were clearly much larger than the singular values corresponding to the noise space. In practice, the singular values of a real EEG epoch do generally not show such a distinct separation between the signal and noise spaces, which is a practical inconvenience when applying the eigenspace-based beamformer.

V. CONCLUSION

The comparison of the quiescent, LCMV and eigenspace-based beamformers applied to simulated EEG signals clearly indicate that the eigenspace-based beamformer is superior to both the quiescent and the LCMV beamformer, as it combines a low white noise gain with a high suppression of interfering sources.

VI. ACKNOWLEDGEMENTS

REFERENCES

[1] P. Boon and M. D'Havé, "Interictal and ictal dipole modelling in patients with refractory partial epilepsy," *Acta Neurologica Scandinavica*, vol. 92, pp. 7–18, 1995.

[2] P. Boon, M. D'Havé, K. Vonck, M. Baulac, T. Vandekerckhove, and J. De Reuck, "Dipole modeling in epilepsy surgery candidates," *Epilepsia*, vol. 38, no. 2, pp. 208–218, 1996.

[3] B. D. Van Veen and K. M. Buckley, "Beamforming: A versatile approach to spatial filtering," *IEEE Acoustics, Speech and Signal Processing Magazine*, vol. 5, pp. 4–24, 1988.

[4] M. E. Spencer, R. M. Leahy, J. C. Mosher, and P. S. Lewis, "Adaptive filters for monitoring localized brain activity from surface potential time series," in *Proceedings of the 26th Asilomar Conference on Signals, Systems and Computers*, pp. 156–161, 1992.

[5] D.-M. Ward, R. D. Jones, P. J. Bones, and G. J. Carroll, "Enhancement of epileptiform activity in the EEG by 3-D adaptive spatial filtering: Simulations and real data," in *Proceedings of 20th Annual International Conference of the IEEE Engineering in Medicine and Biology Society*, vol. 20, part 4/6, (Hong Kong), pp. 2116–2119, 1998.

[6] Y. Salu, L. G. Cohen, D. Rose, S. Sato, C. Kufta, and M. Hallett, "An improved method for localizing electric brain dipoles," *IEEE Transactions on Biomedical Engineering*, vol. 37, pp. 699–705, July 1990.

[7] K. A. Awada, D. R. Jackson, J. T. Williams, D. R. Wilton, S. B. Baumann, and A. C. Papanicolaou, "Computational aspects of finite element modeling in EEG source localization," *IEEE Transactions on Biomedical Engineering*, vol. 44, pp. 736–752, Aug. 1997.

[8] B. Vanrumste, G. Van Hoey, P. Boon, M. D'Havé, and I. Lemahieu, "The need for realistically shaped head models in EEG source analysis," in *ACOMEN'98 Advanced Computational Methods in Engineering*, vol. part2, (Maastricht, The Netherlands), pp. 527–535, 1998.

This page was intentionally left blank